

Voltammetric lability of multiligand complexes. The case of ML_2

Jaume PUY^{*,a}, Joan CECILIA^b, Josep GALCERAN^a, Raewyn M. TOWN^c and Herman P. van LEEUWEN^d

^a Departament de Química, ^b Departament de Matemàtica, Universitat de Lleida (UdL).

Av. Rovira Roure, 191. E-25198 Lleida (Catalonia, Spain).

^c School of Chemistry, The Queen's University of Belfast, Belfast BT9 5AG, U.K

^d Laboratory of Physical Chemistry and Colloid Science, Wageningen University, P.O. Box 8038, Dreijenplein 6, 6703 HB Wageningen (The Netherlands).

Keywords: voltammetry, lability, reaction layer, kinetic currents

*) corresponding author; e-mail: jpuy@quimica.udl.es; fax: (34)973238264

Abstract

The voltammetric lability of a complex system where a metal ion M and a ligand L form the species ML and ML_2 is examined. Together with the rigorous numerical simulation of the problem, two limiting cases are analysed for the overall process $ML_2 \rightarrow M$: (i) the most common case for aqueous complexes where $ML \rightarrow M$ is the kinetically limiting step and (ii) the case where $ML_2 \rightarrow ML$ is limiting. In both cases, analytical expressions for the lability criteria are provided which show good agreement with the results obtained from the rigorous numerical simulation of the problem.

1. Introduction

The speciation of a metal (or any element), i.e. the distribution of its total concentration over a range of physicochemical forms, is long recognised as being important for determining its reactivity, mobility, bioavailability, and toxicity. Rigorous understanding of metal ion speciation in this context must go beyond consideration of the equilibrium distribution of species. A quantitative characterisation of *dynamic* aspects of metal ion speciation, i.e. the kinetic characteristics of interconversion of metal complex species, is required for correct interpretation of data furnished by dynamic analytical techniques [1] (e.g. permeation liquid membranes, diffusive gradients in thin film, voltammetries), and for establishing a rigorous foundation for the relationship between metal speciation and bioavailability [2].

In this context it is useful to introduce the concept of lability which refers to the extent to which the complexes contribute to the metal flux (towards an analytical sensor or a bioaccumulating organism) via dissociation. In a labile system, equilibrium between ML and M is maintained on any relevant spatial scale so that conditions of maximum metal flux arise. For a given surface reaction of the free metal, the lability of a metal complex species indicates its contribution to the supply of uncomplexed metal. Lability criteria have been established for a range of different situations, e.g. geometry and size of the accumulating surface. These criteria allow an a priori evaluation of the contribution of the complex to the metal supply in terms of characteristic parameters of the system: kinetic constants, diffusion coefficients, time scale of the experiment, relevant size of the sensor, bulk concentrations, etc... Note that lability refers to both the properties of the medium and to the geometrical features of the sensing surface.

For dynamic systems, lability criteria are based on the comparison of the relative magnitudes of the actual kinetic metal flux, J_{kin} , to the maximum pure diffusive flux of the complex, J_{dif} ,

[3]. This arises logically from the definition of J_{kin} : this parameter represents the increase of metal flux appearing in the system as compared to that for a system in the absence of complexed species, but with the same free metal concentration (i. e. J_{kin} is the contribution of the complex to the metal supply). The actual J_{kin} is compared with the maximum kinetic flux that could arise in the system (i.e. when the complex is fully labile) which coincides with the maximum purely diffusive flux of the complex, J_{dif} . For the practical application of this comparison, J_{dif} is estimated by means of the diffusion layer approximation while J_{kin} is obtained by means of the classical reaction layer approximation. Based on bulk concentrations, this approach is a simplification that overestimates J_{kin} : the resulting J_{kin} is the maximum kinetic flux attainable because it assumes an unlimited supply of complex, i.e. that no depletion occurs in the diffusion layer. Using this formalism based on bulk solution concentrations, J_{kin} largely outweighs the maximum J_{dif} of ML for fully labile complexes, whilst in the non-labile case the maximum J_{dif} of ML is much larger than J_{kin} . Drastic changes in lability can occur with time, and with spatial scale. The well-known dimensionless lability criterion parameter, L , ($= J_{\text{kin}}/J_{\text{dif}}$) is used to quantify lability for a given system at a given timescale, with $L \gg 1$ for the fully labile case. An inert (static) complex represents the trivial case in which ML does not contribute to the flux.

Until now, lability criteria have been established only for M-L complexes of 1:1 stoichiometry. In this case, the only possible kinetically limiting step is interconversion of ML and M. In many systems, however, complexes of higher ligand stoichiometry, ML_2 , ML_3 , etc. are formed. The formation of free M from complex species ML_i then involves a sequence of dissociation steps. Quantification of the overall interfacial flux of M requires consideration of all equilibria and all association/dissociation rate constants. The present work opens up the field by deriving analytical expressions for the lability criteria for complexes of 1:2

stoichiometry and comparing these with the results of rigorous numerical simulations. Together with the validation of the classical lability criterion, we present a more refined formulation (introducing L^ϕ) in terms of the relevant species concentrations along the reaction layer.

2. Mathematical Formulation

Let us consider the complexation in solution of a metal ion M with a ligand L according to the scheme



under conditions where the free metal species is consumed by some process taking place at an interface in contact with the solution, for instance a reduction to the metal atom M^0 at an electrode surface



The quotients of the rate constants define the stability constants K_i of the complexes,

$$K_i = k_{a,i}/k_{d,i} \quad (4)$$

The ratios of concentrations Q_i are defined as

$$Q_i = \frac{c_{ML_i}}{c_{ML_{i-1}} c_L} \quad (5)$$

and equal K_i if the corresponding equilibrium is attained.

If diffusion towards a stationary planar electrode is the only relevant transport mechanism, the conservation equations read

$$\frac{\partial c_M}{\partial t} = D_M \frac{\partial^2 c_M}{\partial x^2} + k_{d,1} c_{ML} - k_{a,1} c_M c_L \quad (6)$$

$$\frac{\partial c_L}{\partial t} = D_L \frac{\partial^2 c_L}{\partial x^2} + k_{d,1} c_{ML} - k_{a,1} c_M c_L + k_{d,2} c_{ML_2} - k_{a,2} c_{ML} c_L \quad (7)$$

$$\frac{\partial c_{ML}}{\partial t} = D_L \frac{\partial^2 c_{ML}}{\partial x^2} - k_{d,1} c_{ML} + k_{a,1} c_M c_L + k_{d,2} c_{ML_2} - k_{a,2} c_{ML} c_L \quad (8)$$

$$\frac{\partial c_{ML_2}}{\partial t} = D_L \frac{\partial^2 c_{ML_2}}{\partial x^2} - k_{d,2} c_{ML_2} + k_{a,2} c_{ML} c_L \quad (9)$$

where the diffusion coefficients of all species containing L are assumed to equal D_L .

The initial conditions are, as usual,

$$t = 0: \quad c_i(x, 0) = c_i^* \quad i = M, L, ML, ML_2 \quad (10)$$

For limiting diffusion conditions, the boundary value problem is given by

$$x = 0: \quad c_M(0, t) = 0 \quad \left(\frac{\partial c_L}{\partial x} \right)_{x=0} = \left(\frac{\partial c_{ML}}{\partial x} \right)_{x=0} = \left(\frac{\partial c_{ML_2}}{\partial x} \right)_{x=0} = 0 \quad (11)$$

and

$$x = \infty: \quad c_i(\infty, t) = c_i^* \quad i = M, L, ML, ML_2 \quad (12)$$

which expresses semi-infinite diffusion.

Any one of the eqns. (7)-(9) may be eliminated by noticing that

$$c_L + c_{ML} + 2c_{ML_2} = c_{T,L}^* \quad (13)$$

which comes from the fact that no physical phenomenon distorts the initially flat concentration profile of the total ligand concentration and it can be used to determine, for instance, c_{ML_2} once the concentrations c_M , c_L and c_{ML} are known.

The set of Eqs. (6)-(12) defines the concentration profiles of M, L and ML. The solution of this system is cumbersome due to the presence of non-linear equations. As detailed in the Appendix, we use the Galerkin Finite Element Method (GFEM) [4] to solve the spatial distribution of all the species at any time, whereas a finite-difference method is used for the time evolution. We are interested in the metal flux at the electrode surface given by

$$J_M = D_M \left(\frac{\partial c_M}{\partial x} \right)_{x=0} \quad (14)$$

In case of a sufficiently large excess of ligand ($c_L(x,t) \approx c_L^*$), the association reactions become pseudo first-order and we define

$$K_i c_L^* = K_i' = \frac{c_{ML_i}^*}{c_{ML_{i-1}}^*} \quad (15)$$

$$k_{a,i}' = k_{a,i} c_L^* \quad (16)$$

The limiting case of fully labile complexes under excess of ligand allows a simple analytical solution for the metal flux:

$$J_{M, \text{fully labile}} = \sqrt{\frac{\bar{D}}{\pi t}} c_{T,M}^* \quad (17)$$

where

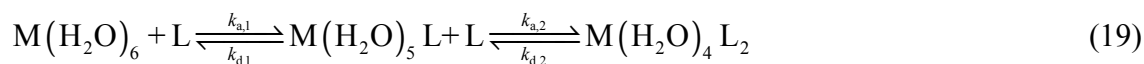
$$\bar{D} \equiv \frac{D_M + D_L K_1' + D_L K_1' K_2'}{1 + K_1' + K_1' K_2'} \quad (18)$$

is the weighted average diffusion coefficient.

3. The case where $ML \rightarrow M$ is the kinetically limiting step in $ML_2 \rightarrow M$

3.1. Volume reactions

The complex formation/dissociation reactions in (1) and (2) are all involved with H_2O binding/release reactions. In terms of inner-sphere bound water, Eqs. (1)-(2) actually imply, for a supposedly constant coordination number of 6:



For a great many types of ligand L, the Eigen mechanism applies to reactions (1) and (2), implying that k_{a1} is determined by the rate of dehydration of the inner coordination sphere of the hydrated metal ion: $M(H_2O)_6 (+ L) \rightarrow M(H_2O)_5 (L)$. Thus, k_{a1} is related to the rate constant for water exchange, k_{-w} , as tabulated for many ions [5]. The constant k_{a2} refers to the removal of the second H_2O from the original $M(H_2O)_6$, which is generally faster than that of the first H_2O . This is mentioned in treatments of the Eigen mechanism, see for instance [5], but also follows from coordination chemical reasoning: the binding of a H_2O molecule in $M(H_2O)_5L$ (formed in an aqueous system containing L) will generally be weaker than in $M(H_2O)_6$ since L is bound more strongly than H_2O . Hence, the common situation is that

$$k_{a1} < k_{a2} \quad (20)$$

The $k_{d,i}$ values are found by combining $k_{a,i}$ values with the thermodynamic stability constants K_i . For any given combination of M and L, with very few exceptions [6]

$$K_1 > K_2 \quad (21)$$

which is consistent with basic coordination chemical principles predicting that the second L is generally bound less strongly than the first one.

On the basis of Eqs. (20) and (21) we can already say something about the dynamic nature of the volume reactions (1) and (2). For instance, if M is in equilibrium with ML in the volume, we have

$$k'_{a,1}t, k_{d,1}t \gg 1 \quad (22)$$

Then, for the reaction (2), we can say that, because of (20), certainly $k'_{a,2}t \gg 1$. Besides, Eq. (21) shows that $k_{d,2}/k_{d,1} > k_{a,2}/k_{a,1}$ and combined with Eq. (20) this gives

$$k_{d,2} > k_{d,1} \quad (23)$$

Thus, if Eq. (22) is obeyed then even more easily is

$$k'_{a,2}t, k_{d,2}t \gg 1 \quad (24)$$

In other words, if in an aqueous M-ML-ML₂ system the equilibrium between M and ML is dynamic, then that between ML and ML₂ is certainly dynamic (indeed, even more so than the former).

3.2. Coupling to interfacial consumption

Returning to the reaction scheme, Eqs. (1) and (2), we now address the question of how ML₂ will kinetically react if M is consumed at an interface which is in contact with the M-ML-ML₂ system. As noted in the introduction, the conventional way to quantify this is to compare the maximum diffusive flux J_{dif} of ML₂ to the interface with the kinetic flux J_{kin} as resulting from the volume dissociation of ML₂ into M, via ML. This limiting diffusive flux of ML₂, J_{dif} , is simply

$$J_{\text{dif}} = \frac{D_L c_{\text{ML}_2}^*}{\delta_{\text{ML}_2}} \quad (25)$$

Formulation of J_{kin} usually derives from reaction layer theory, either or not in combination with the Koutecký-Koryta (KK) approximation [7-9]. In the KK steady-state approximation, the concentration profiles for M, ML and ML_2 in the diffusion layer are spatially divided into a non-labile and labile region, separated by the boundary of the reaction layer (with thickness, μ). The concentrations of ML and ML_2 in the reaction layer are constant. For the ML_2 -ML-M system, the KK approximation thus implies that the gradients of ML_2 and ML (as determined by the kinetically most stable one of the two) in the reaction layer can be taken as negligibly small.

Since we have seen above that $k_{\text{d},2} > k_{\text{d},1}$, Eq. (23), the dissociation of ML to M (+L) is the kinetically limiting step in $\text{ML}_2 \rightarrow \text{M}$. This means that ML is the (relatively stable) intermediate for which in steady-state we can write

$$\frac{dc_{\text{ML}}}{dt} = 0 \quad (26)$$

Rigorously, $\frac{dc_{\text{ML}}}{dt}$ is given by the net yield of the four reactions involved, so that Eq. (26), under excess ligand conditions is approximated by

$$(k'_{\text{a},2} + k_{\text{d},1})c_{\text{ML}} = k_{\text{d},2}c_{\text{ML}_2} + k'_{\text{a},1}c_{\text{M}} \quad (27)$$

Following the reaction layer approach [10], including the proviso that K_1K_2 is sufficiently large, we neglect the reassociation term $k'_{\text{a},1}c_{\text{M}}$. It then follows that the concentration of ML in the reaction layer, c_{ML}^ϕ , is related to the local c_{ML_2} via the rate constants:

$$c_{\text{ML}}^\phi = \frac{k_{\text{d},2}}{k'_{\text{a},2} + k_{\text{d},1}} c_{\text{ML}_2}^\phi \quad (28)$$

Note that $k_{d,1}$ is smaller than $k_{d,2}$, see Eq. (23), and that physically relevant complexation requires that $k'_{a,2} > k_{d,2}$ ($K'_2 > 1$). Thus normally, Eq. (28) approaches

$$c_{ML}^{\phi} \approx \frac{k_{d,2}}{k'_{a,2}} c_{ML_2}^{\phi} = \frac{c_{ML_2}^{\phi}}{K_2 c_L} \quad (29)$$

The kinetic flux J_{kin} is given by the volume dissociation rates of reactions (1) and (2) of which (1) is the rate limiting:

$$R_d = k_{d,1} c_{ML}^{\phi} = \frac{k_{d,1} k_{d,2}}{k'_{a,2} + k_{d,1}} c_{ML_2}^{\phi} \approx k_{d,1} \frac{c_{ML_2}^{\phi}}{K_2 c_L} \quad (30)$$

which implicitly illustrates that the equilibrium between ML_2 and ML is approximately retained, $ML \rightarrow M$ being the rate limiting step. The mean life time of free M is coupled to $k_{a,1} c_L^{\phi}$ and the reaction layer thickness μ , conventionally given by

$$\mu = \frac{D_M^{1/2}}{(k_{a,1} c_L^{\phi})^{1/2}} \quad (31)$$

which retains its classical form because $ML \rightleftharpoons M$ is the kinetically relevant step. Combination of Eqs. (30) and (31) yields the expression for J_{kin}

$$J_{kin} = R_d \mu = k_{d,1} c_{ML}^{\phi} \mu = \frac{k_{d,1} k_{d,2} D_M^{1/2}}{(k'_{a,2} + k_{d,1}) k_{a,1}^{1/2}} c_{ML_2}^{\phi} \quad (32)$$

or approximately,

$$J_{kin} = \frac{k_{d,1} k_{d,2} D_M^{1/2}}{(k'_{a,2} + k_{d,1}) k_{a,1}^{1/2}} c_{ML_2}^{\phi} \approx \frac{k_{d,1} D_M^{1/2}}{K_2 k_{a,1}^{1/2}} c_{ML_2}^{\phi} = \frac{k'_{a,1}{}^{1/2} D_M^{1/2}}{K_1 K_2} c_{ML_2}^{\phi} \quad (33)$$

which differs from the conventional expression for the 1:1 complex by the factor $1/K'_2$ and physically represents the concentration ratio between the relevant M producing species, ML ,

and that which is predominantly present, ML_2 . ML_2 acts as a buffer for ML because $ML_2 \rightleftharpoons ML$ is faster; this effect implies that ML can sustain larger kinetic fluxes than it would by itself. Thus, although the kinetic flux can never be higher than that arising from dissociation of ML, buffering by ML_2 helps to keep J_{kin} as high as possible by maintaining c_{ML}^ϕ . We have the interesting and unusual situation that the kinetic flux of ML may be larger than the diffusive flux of ML. The kinetic flux always obeys $k_{d1}c_{ML}^\phi\mu$, because, so long as c_M^* is sufficiently low, dissociation of ML is the only route for generation of M. The ensuing concentration gradients in ML are instantaneously followed by corresponding gradients in ML_2 (as illustrated in the following sections).

The lability criterion compares the kinetic flux of ML to the maximum total diffusive flux of ML plus ML_2 and thus follows straightforwardly from combination of Eqs. (25) and (32):

$$\frac{J_{kin}}{J_{dif,ML} + J_{dif,ML_2}} = A_{ML_2} \delta_{ML_2} = L \quad (34)$$

with,

$$A_{ML_2} = \frac{k_{d1}D_M^{1/2}}{k_{a1}^{1/2}(1+K_2')D_L} \quad (35)$$

and, for K_2' sufficiently larger than unity

$$A_{ML_2} = \frac{k_{d1}D_M^{1/2}}{k_{a1}^{1/2}K_2'D_L} \quad (36)$$

The lability criteria is

$$L \gg 1 \quad (37)$$

if J_{kin} is evaluated using the bulk concentrations in (32). In this case we denote the resulting value as J_{kin}^* . This is the usual approach taken because it allows straightforward calculation of

J_{kin} from the bulk concentrations (concentrations at the reaction layer are unknown a priori). When ML develops a concentration profile in the diffusion layer, c_{ML}^* is greater than c_{ML}^ϕ and the resulting J_{kin}^* overestimates the real contribution of the complexes to the flux. So, under labile conditions, J_{kin}^* is greater than the maximum kinetic contribution of all the complexes which is given by the maximum total diffusive flux of ML plus ML_2 . It is for this reason that the lability criterion based on bulk concentrations is formulated as $L \gg 1$.

We can develop a more refined approach by using the concentrations at the reaction layer obtained from the rigorous numerical simulation. The resulting J_{kin} , which can be labelled J_{kin}^ϕ , is a good estimation of the contribution of the complexes to the metal flux. We thus formulate L as $J_{\text{kin}}^\phi / J_{\text{dif}} = L^\phi$, with the ensuing criterion for lability being:

$$L^\phi \rightarrow 1 \tag{38}$$

The approach presented above allows generalisation to complexes ML_i for arbitrary values of i .

3.3 Evaluation of the lability criteria, concentration profiles and fluxes

Typical concentration profiles along a chronoamperometric experiment under diffusion limited conditions for the case where $\text{ML} \rightarrow \text{M}$ is the kinetically limiting step in $\text{ML}_2 \rightarrow \text{M}$ are given in Fig 1 for a range of $k_{\text{d},1}$ values.

3.3.1 Inert complexes.

For sufficiently low $k_{\text{d},1}$ (Fig 1a), the system is inert. There is no significant depletion of ML in the diffusion layer and the flux of metal is given by the purely diffusive flux of the free metal with a fixed concentration c_{M}^* in the bulk solution.

$$J_M = \frac{D_M c_M^*}{\delta_M} \quad (39)$$

Due to the excess of ligand and the values of the stability constants, the bulk concentration of free metal in Figs. 1a and 1b is almost zero and the corresponding metal flux at the electrode surface plotted in Fig. 2 is negligible in the inert regime. It should be noticed that J_{kin} , given by (32), does not apply in this situation. This is evidenced by the fact that the effective reaction layer thickness, μ , controlled by $k_{a,1}$ as Eq. (31) indicates, is greater than the effective diffusion layer thickness, δ_M .

3.3.2. Dynamic, non-labile complexes

For certain values of $k_{d,1}$, the system is dynamic and non-labile. The reaction layer thickness μ is now lower than δ_M , and the typical KK-behaviour is clearly demonstrated by the explosion of the Q_1/K_1 values from 1 at distances close to μ as can be seen in Fig. 1b. Conversely, Q_2/K_2 remains close to 1 also for $x < \mu$ indicating the equilibrium behaviour of this step: the overall contribution of ML_2 is limited by the dissociation of ML to M .

In this regime, if c_M^* is negligible, J_M is alternatively given by the effective width of the metal concentration profile or by J_{kin} :

$$J_M = \frac{D_M c_M^*}{\mu} = k_{d,1} c_{ML}^* \mu \quad (40)$$

leading to an increased metal flux with respect to the inert case as can be seen by comparing the values of μ and δ_M (in Fig. 1b, $\delta_M > \mu$ is not shown).

3.3.3. Dynamic, labile complexes

With increasing $k_{d,1}$ values, Figs 1c and 1d, ML dissociates more and more rapidly. Thus greater depletion of ML occurs in approaching equilibrium with M beyond the distance μ , which has been reduced according to Eq. (31). For $x < \mu$, the dissociation process of ML is

not fast enough to maintain equilibrium with M, so Q_1/K_1 explodes from approximately unity (its value for x beyond μ) while c_{ML} and c_{ML_2} maintain an approximately constant value along the reaction layer to reach the prescribed zero slope at the surface as the boundary value problem defines. Conversely, the metal concentration drops to zero as required by the limiting diffusion conditions. Figs. 1c and 1d show that as ML is depleted there is a corresponding parallel depletion of ML_2 all along the profile. As explained above, the dynamic behaviour of $ML_2 \rightleftharpoons ML$ prevents Q_2/K_2 from exploding at distances close to μ .

The role of ML_2 dissociation in buffering ML in the reaction layer is highlighted in Fig. 1c. The dashed line in this Fig. shows the normalised concentration profile of either M or ML in a system with the same c_M^* , c_{ML}^* and kinetic constants as that depicted by the continuous lines in the figure, but without ML_2 (a sufficiently low k_{a2} value has been chosen to obtain a negligible $c_{ML_2}^*$; $c_{T,M}^*$ and $c_{T,L}^*$ have been respectively chosen as $c_M^* + c_{ML}^*$ and $c_L^* + c_{ML}^*$ of the system depicted by the continuous lines). The dashed line accounts for both M and ML concentration profiles indicating that there is equilibrium in this system along all the profile. The comparison of M and ML concentration profiles (i.e. the continuous and dashed lines for each species) provides clear evidence for the buffering effect of ML_2 : (i) when there is no ML_2 the concentration profile of M extends further into the solution since neither ML (whose c_{ML}^* is very low) nor the nonexistent ML_2 can buffer the concentration of M, (ii) the slope of the metal concentration profile at the electrode surface indicates that the metal flux decreases when ML_2 is not present, and (iii) the values reached by c_{ML}^0 are larger when there is ML_2 . In spite of the increased flux for the case with ML_2 , the system without ML_2 appears to be more labile (as seen through the practically null value of c_{ML}^0). This result is consistent with: (i) the increase in A_{ML_2} given by (35) when ML_2 is absent, because K_2' is missing in the denominator

of (35), and (ii) the decrease of the total maximum diffusional flux of $ML + ML_2$ in the absence of ML_2 because in the case under consideration ML_2 is the predominant metal species in bulk solution.

Together with the metal flux at the electrode surface, J_M , obtained from the numerical solution of the concentration profiles, Fig. 2 plots the approximate J_M value obtained from the analytical expression Eq. (32). This value is labelled J_{kin}^* since we use c_L^* and $c_{ML_2}^*$ instead of the c_L^ϕ and the $c_{ML_2}^\phi$ values appearing in Eq. (32), and is depicted in Fig. 2 as a dashed line. A good agreement between J_M and J_{kin}^* is seen within the inert or dynamic non-labile regimes (for values of the kinetic constant $k_{a,1}$ up to $10^5 \text{ mol}^{-1} \text{ m}^3 \text{ s}^{-1}$ in Fig. 2). In the labile regime, J_{kin}^* is greater than the maximum J_M , as explained above, and the inequality $L \gg 1$ applies.

The transition to the labile regime is recognised by the decrease of ML concentration in the reaction layer (which can be monitored through the concentration at the electrode surface c_{ML}^0). The decrease in c_{ML}^0 is immediately followed by a parallel decrease in $c_{ML_2}^0$ as is shown in Fig 2 or going from Fig 1b to Fig 1c. In fact, despite the equilibrium nature of the step $ML_2 \rightleftharpoons ML$, $c_{ML_2}^0$ cannot decrease unless sufficiently labile conditions for $ML \rightleftharpoons M$ are reached. In the course of this transition, the metal flux, J_M , increases due to the contribution of the metal released by the dissociation of both ML and ML_2 but J_{kin}^* explodes due to the use of $c_{ML_2}^*$ instead of $c_{ML_2}^\phi$ in Eq. (32). Fig. 1d clearly shows that $c_{ML_2}^*$ differs from the steady-state $c_{ML_2}^\phi$ value in the reaction layer by a factor of approximately 3 (this being the factor responsible for the explosion of J_{kin}^* with respect to J_M). If $c_{ML_2}^*$ is replaced by $c_{ML_2}^0$,

the resulting J_{kin} value, labelled as J_{kin}^{ϕ} , shows good agreement with J_{M} up to $k_{a1} = 10^8 \text{ mol}^{-1} \text{ m}^3 \text{ s}^{-1}$ (see Fig. 2).

J_{M} in the labile regime can be compared to the limiting value given by Eq. (17). For data of Fig. 2, Eq. (17) yields $J_{\text{M}, \text{fully labile}} = 2.53 \times 10^{-6} \text{ mol m}^{-2} \text{ s}^{-1}$, depicted as bullets at the right-hand side of fig. 2, and in good agreement with J_{M} in the labile regime, the small divergence being due to the impact of the finite ligand-to-metal ratio. For the data of Fig. 2, J_{M} in the labile regime is also close to the diffusional flux of ML_2 given by Eq. (25), ($2.46 \times 10^{-6} \text{ mol m}^{-2} \text{ s}^{-1}$), since almost all the metal is present in the solution as ML_2 . As expected, the maximum J_{kin} is then the maximum total diffusive flux of ML plus ML_2 which justifies its use in the lability criterion (34).

If the excess of ligand is reduced, for instance with $c_{\text{T,L}}^*$ only 3 times $c_{\text{T,M}}^*$ in Fig. 3, the development of the concentration profiles of ML and ML_2 in the transition to the labile regime leads to the concomitant development of a ligand concentration profile, with c_{L} increasing towards the electrode surface. In this case, the divergence between J_{M} and J_{kin}^* is more critical and only the value of J_{kin}^{ϕ} (given by Eq. (32)) reproduces with good accuracy J_{M} in the labile limit, which is eventually close to the corresponding value given by Eq. (17) (see bullets in Fig. 3). The extension of the reaction layer concepts to non ligand excess conditions has been discussed before [10]. Fig. 3 also shows a small discrepancy between J_{M} and J_{kin}^{ϕ} at very low values of the kinetic constants $k_{a,1}$, $k_{d,1}$. This discrepancy results from the diffusional flux associated with the free metal in solution. Actually, on increasing the stability

constant (see Fig 4), c_M^* decreases, the corresponding flux becomes more and more negligible, and J_M is again well reproduced by J_{kin} .

All cases show the correctness of the lability criterion, Eq. (34), as evidenced by the increase in J_{kin} or the increase of the lability parameter, A_{ML_2} , just when c_{ML}^0 drops to zero. Thus, Eq. (34) can be used as the lability criterion for the case where $ML \rightarrow M$ is the kinetically limiting step in the overall process $ML_2 \rightarrow M$. This expression will hold even if A_{ML_2} is calculated with bulk concentrations, or there is a non-negligible bulk free metal concentration. The criterion (34) holds even for $K_2 > K_1$ (a much less common situation) so long as $ML \rightarrow M$ is the kinetically limiting step in the $ML_2 \rightarrow M$ process, as can be seen from the reasoning leading to Eq. (34).

4. The case where $ML_2 \rightarrow ML$ is the kinetically limiting step in $ML_2 \rightarrow M$

4.1 Lability criterion

For the sake of completeness of the theory, we also consider the case where the dissociation of ML_2 into ML and L is slower than that of ML into M and L , i.e. the case

$$k_{d1} > k_{d2} \quad (41)$$

together with the assumption concerning the stability constants

$$K_2', K_1' \gg 1 \quad (42)$$

Under these conditions, the kinetics of the step $ML_2 \rightleftharpoons ML$ are relevant in the problem since almost all the metal is in the form ML_2 in the bulk solution. Only if $K_2', K_1' \gg 1$ will the expression for the kinetic metal flux arising from the dissociation of ML_2 satisfactorily approach the metal flux.

The kinetic contribution comes from the step $ML_2 \rightarrow ML$ since the remaining dissociation step, $ML \rightarrow M$, is not rate limiting, and

$$R_d = k_{d,2}c_{ML_2}^\phi \quad (43)$$

Since ML_2 is the kinetically relevant complex, we can approach this case by considering the sum $(M + ML)$ as a new formal species assuming that the interchanging process $ML \rightleftharpoons M$ is so fast that equilibrium conditions are instantaneously reached at any relevant spatial position. The mean life-time of this new formal species $(M + ML)$ will then be determined by $R_{a,2}$ which can be written as (under excess ligand conditions)

$$R_{a,2} = k_{a,2}c_{ML}^\phi c_L^\phi = k_{a,2} \frac{K_1'}{1 + K_1'} (c_M^\phi + c_{ML}^\phi) c_L^\phi = k_{a,2}^{app} (c_M^\phi + c_{ML}^\phi) \quad (44)$$

where $k_{a,2}^{app}$ (defined as $k_{a,2}' \frac{K_1'}{1 + K_1'}$) is the apparent association constant for $(M + ML)$.

Thus, the mean life-time of $M+ML$ is coupled to $k_{a,2}^{app}$ and the reaction layer thickness, μ , can be expressed in the conventional way

$$\mu = \left(\frac{D_1}{k_{a,2}^{app}} \right)^{1/2} = \frac{D_1^{1/2} (1 + K_1')^{1/2}}{(k_{a,2}' K_1')^{1/2}} \quad (45)$$

where

$$D_1 = D_M \frac{1}{1 + K_1'} + D_{ML} \frac{K_1'}{1 + K_1'} \quad (46)$$

is the diffusion coefficient of the formal species $(M+ML)$ obtained as the average of the M and ML diffusion coefficients.

The kinetic flux then follows

$$J_{\text{kin}} = R_d \mu = k_{d,2} c_{\text{ML}_2}^\phi \mu = \frac{k_{a,2}^{1/2} D_1^{1/2} (1 + K_1')^{1/2}}{K_2' K_1'^{1/2}} c_{\text{ML}_2}^\phi \quad (47)$$

and the lability criterion follows straightforwardly from the comparison of J_{kin} given by Eqn. (47) with the maximum kinetic contribution. As the condition $K_2', K_1' \gg 1$ implies a negligible c_{ML}^* , the diffusional flux of ML is negligible and the maximum kinetic flux is $J_{\text{dif,ML}_2}$. Then

$$\frac{J_{\text{kin}}}{J_{\text{dif,ML}_2}} = A_{\text{ML}_2} \delta_{\text{ML}_2} = L \quad (48)$$

with A_{ML_2} now given by

$$A_{\text{ML}_2} = \frac{k_{a,2}^{1/2} D_1^{1/2} (1 + K_1')^{1/2}}{K_2' K_1'^{1/2} D_{\text{ML}_2}} \quad (49)$$

becoming

$$L \gg 1 \quad (50)$$

if J_{kin} is evaluated using the bulk concentrations in (47), while

$$L^\phi \rightarrow 1 \quad (51)$$

if J_{kin} is evaluated using the reaction layer concentrations in (47). Comments on these equations are parallel to those concerning Eqns. (37) and (38). Generalisation of this approach to complexes ML_i for arbitrary values of i is straightforward.

4.2 Evaluation of the lability criteria, concentration profiles and fluxes

Figs. 5 show the concentration profiles of M, ML and ML_2 for cases (with various k_{d2} values) where the dissociation step $\text{ML}_2 \rightarrow \text{ML}$ limits the kinetic production of free metal ion.

For sufficiently low $k_{d,2}$ (Fig. 5a), ML follows the depletion of M due to the lability of ML although ML_2 is not able to dissociate fast enough for $x < \mu$ given by Eq. (45) where Q_2/K_2 explodes. Note that the normalisation factors for the concentrations in Fig. 5 magnify the gradients of M and ML since, in fact, their bulk concentrations are much lower than that of ML_2 .

On increasing $k_{d,2}$, Fig. 5a to Fig. 5c, the reaction layer thickness decreases and the explosion of Q_2/K_2 takes place closer to the electrode as predicted by Eq. (45) and the profile of ML_2 becomes increasingly steeper. As we are not in conditions of excess ligand, a ligand concentration profile also develops in Figs. 5, with c_L increasing towards the electrode surface. When the ligand concentration is almost constant, the normalised profiles of M and ML converge (see Fig. 5a over the entire spatial range). This is a simple consequence of the lability of ML which ensures that the concentration ratio of ML to M is constant along the profile and equal to K_1' , or equivalently, $c_M / c_M^* = c_{ML} / c_{ML}^*$

When the increase of the ligand concentration profile becomes more pronounced (Fig. 5b and 5c), the normalised profiles of ML and M diverge due to the local changes in c_L (while Q_1 continues to equal K_1).

According to Fig. 6, the metal flux obtained by the rigorous numerical simulation of the problem, J_M , is generally well described by J_{kin}^ϕ , i.e. the value resulting from Eq. (47) obtained by using c_L^0 and $c_{ML_2}^0$ instead of c_L^ϕ and $c_{ML_2}^\phi$. As can be seen in Fig. 6, the agreement between J_M and J_{kin}^ϕ holds, as expected, so long as the key condition (41) holds, i.e. so long as $ML_2 \rightarrow ML$ is the kinetically limiting step in $ML_2 \rightarrow M$ up to $k_{a,2}$ around 10^7

$\text{mol}^{-1} \text{m}^3 \text{s}^{-1}$. The transition to the labile regime, recognised by the decrease of $c_{\text{ML}_2}^\phi$ to zero, is then well indicated by the lability criterion, Eq. (48).

On decreasing the ratio K_2/K_1 , Fig. 7, the lability parameter $J_{\text{kin}}/J_{\text{dif}}$ still reproduces correctly the transition from non-labile to labile regime for the ML_2 complex. However, the metal flux is not well reproduced by Eq. (47) due to the presence of a non-negligible bulk concentration of ML which is not modelled by (47), but which does contribute to the metal flux. The lability of ML is illustrated in Figs. 6 and 7 by the low value of c_{ML}^0 in all the $k_{a,2}$ range covered.

5. Conclusions

The metal flux at an interface in contact with a solution containing complexes of stoichiometry ML and ML_2 is examined in detail. The concept of lability is formulated as a property of the system as a whole, regardless of the mechanisms involved. For aqueous metal complexes, almost without exception, $K_1 > K_2$, and hence $k_{d,1} < k_{d,2}$. Thus, the step $\text{ML} \rightarrow \text{M}$ is the kinetically limiting one in the overall reaction $\text{ML}_2 \rightarrow \text{ML} \rightarrow \text{M}$ under conditions of consumption of M at a surface, e.g. an electrode or a biointerface. That is, if the equilibrium between M and ML is dynamic, then that between ML and ML_2 is certainly also dynamic. ML_2 effectively acts as a kinetically unlimited buffer of ML in the reaction layer, and we have the unusual situation of the kinetic flux of ML being potentially larger than its diffusive flux.

When $\text{ML} \rightarrow \text{M}$ is the kinetically limiting step in $\text{ML}_2 \rightarrow \text{M}$, the reaction layer concept allows an approximate analytical expression to be derived for the metal flux, together with a lability criterion, by comparing the kinetic metal flux with the maximum total diffusive flux of ML

plus ML_2 . The accuracy of the corresponding expressions has been checked with the rigorous numerical simulation of the problem. The metal flux is well reproduced by the reaction layer concept when the concentrations at the reaction layer are used, these values differ from the bulk concentrations when the complexes are semi-labile or there is no excess of ligand. However, even in these cases, the lability criterion based on bulk concentrations can be used to predict the critical conditions required to reach labile behaviour.

For the less common case where $ML_2 \rightarrow ML$ is the kinetically limiting step in $ML_2 \rightarrow M$, the reaction layer concept has allowed approximate analytical expressions to be obtained for the metal flux when $K'_2, K'_1 \gg 1$. The lability criterion has then been obtained by comparison of this flux with the maximum diffusional flux of ML_2 . The results obtained are in good agreement with numerical simulations.

Symbols and abbreviations

symbol	meaning	units	equation
A, B	Finite Element Method (FEM) matrices	$s^{-1/2}$ and $s^{-1/2}$	(A16)
c_i	concentration of species i (M, L, ML, ML_2)	mol m^{-3}	(6)
D_i	diffusion coefficient of species i (M, L, ML, ML_2)	$\text{m}^2 \text{s}^{-1}$	(6)-(9)
\bar{D}	average diffusion coefficient	$\text{m}^2 \text{s}^{-1}$	(18)

f_1, f_2	kinetic generation terms	$\text{mol m}^{-3}\text{s}^{-1}$	(A1)
$J_{M, \text{fully labile}}$	fully labile flux	$\text{mol m}^{-2}\text{s}^{-1}$	(17)
J_{dif}	limiting diffusive flux of ML_2	$\text{mol m}^{-2}\text{s}^{-1}$	(25)
J_{kin}	kinetic flux	$\text{mol m}^{-2}\text{s}^{-1}$	(33), (47)
J_M	arriving flux of M	$\text{mol m}^{-2}\text{s}^{-1}$	(14)
K_i	stability constant of complex ML_i	$\text{m}^3\text{mol}^{-1}$	(4)
$k_{a,i}$	complex formation rate constant for complex i	$\text{m}^3\text{mol}^{-1}\text{s}^{-1}$	(4)
$k_{d,i}$	complex dissociation rate constant for complex i	s^{-1}	(4)
K'_i	product of stability constant and ligand concentration for complex i	none	(15)
$k'_{a,i}$	product of complex formation rate constant and ligand concentration for complex i	none	(16)
L	Lability parameter	none	(34)
p	vector of gradients	$\text{s}^{-1/2}$	(A9)
Q_i	ratio of concentrations for complex ML_i	$\text{m}^3\text{mol}^{-1}$	(5)
q_i	normalised concentration	none	(A6)
$R_{a,2}$	kinetic disappearance of M	$\text{mol m}^{-3}\text{s}^{-1}$	(43)
R_d	kinetic generation of M	$\text{mol m}^{-3}\text{s}^{-1}$	(30)
t	time	s	(6)
x	spatial coordinate	m	(6)
z	new coordinate	$\text{s}^{1/2}$	(A6)

$\delta \equiv \delta_{ML_2}$	diffusion layer thickness	m	(25)
ε	normalised diffusion coefficient	none	(A6)
Λ	lability parameter	m^{-1}	(34), (48)
μ	reaction layer thickness	m	(31)

SUPERSCRIPTS AND SUBSCRIPTS

* bulk solution

0 electrode (or bioactive) surface

ϕ within the reaction layer

Appendix

The rigorous numerical solution of the system stated by Eqs. (6)-(12) is done by solving the problem

$$\left. \begin{aligned} \frac{\partial c_M}{\partial t} &= D_M \frac{\partial^2 c_M}{\partial x^2} + f_1 \\ \frac{\partial c_L}{\partial t} &= D_L \frac{\partial^2 c_L}{\partial x^2} + f_1 + f_2 \\ \frac{\partial c_{ML}}{\partial t} &= D_L \frac{\partial^2 c_{ML}}{\partial x^2} - f_1 + f_2 \\ f_1 &= k_{d,1} c_{ML} - k_{a,1} c_M c_L \\ f_2 &= \frac{k_{d,2}}{2} (c_{T,L}^* - c_L - c_{ML}) - k_{a,2} c_{ML} c_L \end{aligned} \right\} \quad (A1)$$

with initial conditions and boundary conditions at $x \rightarrow \infty$ given by

$$c_i(x, 0) = c_i(\infty, t) = c_i^* \quad i = M, L, ML \quad (A2)$$

$$f_j(x, 0) = f_j(\infty, t) = 0 \quad j = 1, 2 \quad (A3)$$

and boundary conditions at $x = 0$

$$c_M(0, t) = 0 \quad (A4)$$

$$\left(\frac{\partial c_L(x, t)}{\partial x} \right)_{x=0} = \left(\frac{\partial c_{ML}(x, t)}{\partial x} \right)_{x=0} = 0 \quad (A5)$$

Using the change of variables

$$q_i = \frac{c_i}{c_i^*}, \quad z = \frac{x}{\sqrt{D_M}}, \quad \varepsilon = \frac{D_L}{D_M} \quad (A6)$$

the problem becomes

$$\left. \begin{aligned}
 \frac{\partial q_M}{\partial t} &= \frac{\partial^2 q_M}{\partial z^2} + \frac{f_1}{c_M^*} \\
 \frac{\partial q_L}{\partial t} &= \varepsilon \frac{\partial^2 q_L}{\partial z^2} + \frac{f_1 + f_2}{c_L^*} \\
 \frac{\partial q_{ML}}{\partial t} &= \varepsilon \frac{\partial^2 q_{ML}}{\partial z^2} + \frac{-f_1 + f_2}{c_{ML}^*} \\
 f_1 - k_{d,1} c_{ML}^* q_{ML} + k_{a,1} c_M^* c_L^* q_M q_L &= 0 \\
 f_2 - \frac{k_{d,2}}{2} (c_{T,L}^* - c_L^* q_L - c_{ML}^* q_{ML}) + k_{a,2} c_{ML}^* c_L^* q_{ML} q_L &= 0
 \end{aligned} \right\} \quad (A7)$$

and the initial and boundary value problem

$$\left. \begin{aligned}
 q_i(z, 0) &= q_i(\infty, t) = 1 \quad i = M, L, ML \\
 f_j(z, 0) &= f_j(\infty, t) = 0 \quad j = 1, 2 \\
 q_M(0, t) &= 0 \\
 \left(\frac{\partial q_L}{\partial z} \right)_{z=0} &= \left(\frac{\partial q_{ML}}{\partial z} \right)_{z=0} = 0
 \end{aligned} \right\} \quad (A8)$$

The discretisation of the spatial part is carried out using a mesh $(0, z_1, \dots, z_{N-1}, z_N)$ adapted to the problem [10-13]. Indeed, if $h_i = z_i - z_{i-1}$, the values of these steps h_i increase, for example, from 10^{-4} to 10^{-1} , in units of $1/\sqrt{D_M}$ increasing the number or spatial points so that the distance between them is reduced close to the electrode where the gradient of the unknown functions are expected to be greater. The value of the last position of the mesh, z_N , is large enough to consider that the unknown concentrations reach the bulk values on this position. Over this mesh, we define the following N -dimensional vectors:

$$\vec{p}(t) = \left(\left(\frac{\partial q_M}{\partial z} \right)_{z=0}, 0, \dots, 0 \right) \quad (A9)$$

$$\vec{q}_M(t) = (0, q_{M1}(t), \dots, q_{MN-1}(t)) \quad (A10)$$

$$\vec{q}_L(t) = (q_{L0}(t), q_{L1}(t), \dots, q_{LN-1}(t)) \quad (A11)$$

$$\vec{q}_{ML}(t) = (q_{ML0}(t), q_{ML1}(t), \dots, q_{MLN-1}(t)) \quad (A12)$$

$$\vec{f}_1(t) = (f_{10}(t), f_{11}(t), \dots, f_{1N-1}(t)) \quad (A13)$$

$$\vec{f}_2(t) = (f_{20}(t), f_{21}(t), \dots, f_{2N-1}(t)) \quad (A14)$$

$$\vec{\beta} = (0, \dots, 0, -1/h_N) \quad (A15)$$

where $q_{ij}(t) = q_i(z_j, t)$ and $f_{ij}(t) = f_i(z_j, t)$. For the temporal part we use a regular discretisation $(0, t_1, \dots, t_j, \dots)$ where $t_j = j \cdot \Delta t$.

Applying the FEM [4,10-14] to the spatial part and the Inverse-Euler scheme to the temporal part [15], we obtain the following system of equations:

$$\left. \begin{aligned} & \left(\frac{1}{\Delta t} A + B \right) \vec{q}_M(t + \Delta t) + \vec{p}(t + \Delta t) - \frac{1}{c_M^*} A \vec{f}_1(t + \Delta t) - \frac{1}{\Delta t} A \vec{q}_M(t) + \vec{\beta} = 0 \\ & \left(\frac{1}{\Delta t} A + \varepsilon \cdot B \right) \vec{q}_L(t + \Delta t) - \frac{1}{c_L^*} A \vec{f}_1(t + \Delta t) - \frac{1}{c_L^*} A \vec{f}_2(t + \Delta t) - \frac{1}{\Delta t} A \vec{q}_L(t) + \varepsilon \cdot \vec{\beta} = 0 \\ & \left(\frac{1}{\Delta t} A + \varepsilon \cdot B \right) \vec{q}_{ML}(t + \Delta t) + \frac{1}{c_{ML}^*} A \vec{f}_1(t + \Delta t) - \frac{1}{c_{ML}^*} A \vec{f}_2(t + \Delta t) - \frac{1}{\Delta t} A \vec{q}_{ML}(t) + \varepsilon \cdot \vec{\beta} = 0 \\ & f_{1i}(t + \Delta t) - k_{d,1} c_{ML}^* q_{MLi}(t + \Delta t) + k_{a,1} c_M^* c_L^* q_{Mi}(t + \Delta t) q_{Li}(t + \Delta t) = 0 \\ & f_{2i}(t + \Delta t) - \frac{k_{d,2}}{2} (c_{T,L}^* - c_L^* q_{Li}(t + \Delta t) - c_{ML}^* q_{MLi}(t + \Delta t)) + k_{a,2} c_{ML}^* c_L^* q_{MLi}(t + \Delta t) q_{Li}(t + \Delta t) = 0 \end{aligned} \right\}$$

$$i = 0, \dots, N-1 \quad (A16)$$

where A and B are the usual symmetric matrices that appear in the application of the FEM method [11]:

Acknowledgements

The authors gratefully acknowledge support of this research by the European Commission under contract EVK1-CT-2001-00086 (BIOSPEC; RTD Programme "Preserving the Ecosystem" (Key Action Sustainable Management and Quality of Water)), and by the Spanish Ministry of Education and Science (DGICYT: Projects BQU2003-9698 and BQU2003-07587) and the "Comissionat d'Universitats i Recerca de la Generalitat de Catalunya".

Figure captions

1.- Normalised concentration profiles, c_i/c_i^* , of M (\diamond), ML (Δ), ML₂ (\times) and L () referred to the left ordinate axis and Q_1/K_1 (*) and Q_2/K_2 (o), referred to the right ordinate axis as a function of the distance to the electrode surface measured as $x/\sqrt{D_M t}$. Parameters: $k_{a,1}=1 \text{ mol}^{-1} \text{ m}^3 \text{ s}^{-1}$, $k_{d,1}=0.01 \text{ s}^{-1}$, (Fig. 1a); $k_{a,1}=10^4 \text{ mol}^{-1} \text{ m}^3 \text{ s}^{-1}$, $k_{d,1}=10^2 \text{ s}^{-1}$ (Fig. 1b); $k_{a,1}=10^7 \text{ mol}^{-1} \text{ m}^3 \text{ s}^{-1}$, $k_{d,1}=10^5 \text{ s}^{-1}$ (Fig. 1c) and $k_{a,1}=10^8 \text{ mol}^{-1} \text{ m}^3 \text{ s}^{-1}$, $k_{d,1}=10^6 \text{ s}^{-1}$ (Fig. 1d). The vertical dashed line denotes the thickness of the reaction layer (μ) given by (31) or that of the diffusion layer thickness ($\delta_M = \sqrt{\pi D_M t}$). The dashed line in Fig. 1c corresponds to the concentration profile of either M or ML for the hypothetical case of absence of ML₂ with parameters (kinetic constants, bulk M and ML concentrations, diffusion coefficients) as in the continuous lines of Fig. 1c, but different total metal and ligand concentrations (see text for details). Other parameters are: $c_{T,M}^* = 0.1 \text{ mol m}^{-3}$, $c_{T,L}^* = 1 \text{ mol m}^{-3}$, $k_{a,2} = 10^8 \text{ mol}^{-1} \text{ m}^3 \text{ s}^{-1}$, $k_{d,2} = 2 \times 10^6 \text{ s}^{-1}$, $D_M = 1 \times 10^{-9} \text{ m}^2 \text{ s}^{-1}$, $D_{ML} = D_L = 1 \times 10^{-10} \text{ m}^2 \text{ s}^{-1}$, $t = 0.05 \text{ s}$.

2.- Metal flux at the electrode surface, J_M (continuous line), the kinetic flux, J_{kin}^* (short dashed line) and J_{kin}^ϕ (long dashed line), referred to the right ordinate axis and c_{ML}^0/c_{ML}^* and $c_{ML_2}^0/c_{ML_2}^*$, both referred to the left ordinate axis as functions of the association kinetic constant $\log(k_{a,1}/\text{mol}^{-1} \text{ m}^3 \text{ s}^{-1})$. J_{kin}^ϕ is calculated via (32) using the values of c_L^0 and $c_{ML_2}^0$ obtained from the numerical solution as approximate values for c_L^ϕ and $c_{ML_2}^\phi$. J_{kin}^* is obtained using c_L^* and $c_{ML_2}^*$ instead of c_L^ϕ and $c_{ML_2}^\phi$ appearing in (32). In each point, $k_{d,1}$ takes the

value required to maintain a fixed K_1 equal to $10^2 \text{ mol}^{-1} \text{ m}^3$. The horizontal bullets on the right side indicate the fully labile case given by Eq. (17). The rest of parameters as in Fig 1.

3.- Metal flux at the electrode surface, J_M (continuous line), the kinetic flux, J_{kin}^* (short dashed line) and J_{kin}^ϕ (long dashed line), referred to the right ordinate axis and c_{ML}^0/c_{ML}^* and $c_{ML_2}^0/c_{ML_2}^*$, both referred to the left ordinate axis as functions of the association kinetic constant $\log(k_{a1}/\text{mol}^{-1} \text{ m}^3 \text{ s}^{-1})$. J_{kin}^* and J_{kin}^ϕ are obtained as described in Fig. 2. Parameters: $c_{T,M}^* = 0.1 \text{ mol m}^{-3}$, $c_{T,L}^* = 0.3 \text{ mol m}^{-3}$. The rest of parameters as in Fig 2.

4.- Metal flux at the electrode surface, J_M (continuous line), the kinetic flux, J_{kin}^* (short dashed line) and J_{kin}^ϕ (long dashed line), referred to the right ordinate axis and c_{ML}^0/c_{ML}^* and $c_{ML_2}^0/c_{ML_2}^*$, both referred to the left ordinate axis as functions of the association kinetic constant $\log(k_{a1}/\text{mol}^{-1} \text{ m}^3 \text{ s}^{-1})$. J_{kin}^* and J_{kin}^ϕ are obtained as described in Fig. 2. Parameters: $c_{T,M}^* = 0.1 \text{ mol m}^{-3}$, $c_{T,L}^* = 0.3 \text{ mol m}^{-3}$, $k_{a,2} = 10^8 \text{ mol}^{-1} \text{ m}^3 \text{ s}^{-1}$, $k_{d,2} = 10^7 \text{ s}^{-1}$ and in each point, k_{d1} takes the value required to maintain a fixed K_1 equal to $10^4 \text{ mol}^{-1} \text{ m}^3$. The rest of parameters as in Fig. 2.

5.- Normalised concentration profiles, c_i/c_i^* , of M (\diamond), ML (Δ), ML_2 (\times) and L () referred to the left ordinate axis and Q_1/K_1 (*) and Q_2/K_2 (o), referred to the right ordinate axis as a function of the distance to the electrode surface measured as $x/\sqrt{D_M t}$. Parameters: $c_{T,M}^* = 0.1 \text{ mol m}^{-3}$, $c_{T,L}^* = 0.3 \text{ mol m}^{-3}$, $k_{a,1} = 10^8 \text{ mol}^{-1} \text{ m}^3 \text{ s}^{-1}$, $k_{d,1} = 10^7 \text{ s}^{-1}$ and $k_{a,2} = 10^3 \text{ mol}^{-1} \text{ m}^3 \text{ s}^{-1}$, $k_{d,2} = 1 \text{ s}^{-1}$, (Fig. 5a); $k_{a,2} = 10^4 \text{ mol}^{-1} \text{ m}^3 \text{ s}^{-1}$, $k_{d,2} = 10^1 \text{ s}^{-1}$ (Fig. 5b); $k_{a,2} = 10^5 \text{ mol}^{-1} \text{ m}^3 \text{ s}^{-1}$, $k_{d,2} = 10^2$

s^{-1} (Fig. 5c). The vertical dashed line denotes the thickness of the reaction layer, μ , in dimensionless units, given by (45). Other parameters as in Fig. 1.

6.- Metal flux at the electrode surface, J_M (continuous line), the kinetic flux, J_{kin}^* (long dashed line) and J_{kin}^ϕ (short dashed line), referred to the right ordinate axis and c_{ML}^0/c_{ML}^* and $c_{ML_2}^0/c_{ML_2}^*$, both referred to the left ordinate axis as functions of the association kinetic constant $\log(k_{a,2}/\text{mol}^{-1}\text{m}^3\text{s}^{-1})$. J_{kin}^ϕ is calculated via (47) using the values of c_L^0 and $c_{ML_2}^0$ obtained from the numerical solution as approximate values for c_L^ϕ and $c_{ML_2}^\phi$. J_{kin}^* is obtained using c_L^* and $c_{ML_2}^*$ instead of c_L^ϕ and $c_{ML_2}^\phi$ appearing in (47). In each point, $k_{d,2}$ takes the value required to maintain a fixed K_2 equal to $10^3\text{mol}^{-1}\text{m}^3$. The horizontal bullets on the right side indicate the fully labile case given by eqn. (17). The rest of parameters as in Fig. 5.

7.- Metal flux at the electrode surface, J_M (continuous line), the kinetic flux, J_{kin}^* (short dashed line) and J_{kin}^ϕ (long dashed line), referred to the right ordinate axis and c_{ML}^0/c_{ML}^* and $c_{ML_2}^0/c_{ML_2}^*$, both referred to the left ordinate axis as functions of the association kinetic constant $\log(k_{a,2}/\text{mol}^{-1}\text{m}^3\text{s}^{-1})$. J_{kin}^* and J_{kin}^ϕ are obtained as described in caption of Fig. 6. In each point, $k_{d,2}$ takes the value required to maintain a fixed K_2 equal to $10^2\text{mol}^{-1}\text{m}^3$. The rest of parameters as in Fig. 6.

Reference List

- [1] J.Buffle, G.Horvai, (Eds.), In Situ Monitoring of Aquatic Systems. Chemical Analysis and Speciation. Vol. 6. IUPAC Series on Analytical and Physical Chemistry of Environmental Systems. J. Buffle, H. P. van Leeuwen (Series Eds.), John Wiley & Sons, Chichester, 2000.
- [2] H.P.van Leeuwen, W.Köster, (Eds.), Physicochemical Kinetics and Transport at Biointerfaces. Vol. 9. IUPAC Series on Analytical and Physical Chemistry of Environmental Systems. J. Buffle, H. P. van Leeuwen (Series Eds.), John Wiley & Sons, Chichester, 2004.
- [3] H.P.van Leeuwen, *Electroanal.* 13 (2001) 826.
- [4] A.R.Mitchell, D.F.Griffiths, *The Finite Element Method in Partial Differential Equations*, Wiley, New York, 1987.
- [5] F.M.M.Morel, J.G.Hering, *Principles and Applications of Aquatic Chemistry*, John Wiley, New York, 1993, Chapter 6, p. 319.
- [6] K.J.Powell, *SCDatabase*, Academic Software, United Kingdom, 2000.
- [7] J.Heyrovský, J.Kuta, *Principles of Polarography*, Academic Press, New York, 1966.
- [8] J.Koutecký, J.Koryta, *Electrochim. Acta* 3 (1961) 318.
- [9] J.Koryta, J.Dvorak, L.Kavan, *Principles of Electrochemistry*, Second ed. John Wiley, Chichester, 1993.
- [10] H.P.van Leeuwen, J.Puy, J.Galceran, J.Cecília, *J. Electroanal. Chem.* 526 (2002) 10.
- [11] J.Cecília, J.Galceran, J.Salvador, J.Puy, F.Mas, *Int. J. Quantum Chem.* 51 (1994) 357.
- [12] J.Puy, J.Galceran, J.Salvador, J.Cecília, M.S.Diaz-Cruz, M.Esteban, F.Mas, *J. Electroanal. Chem.* 374 (1994) 223.
- [13] J.Puy, M.Torrent, J.Monné, J.Cecília, J.Galceran, J.Salvador, J.L.Garcés, F.Mas, F.Berbel, *J. Electroanal. Chem.* 457 (1998) 229.
- [14] T.J.R.Hughes, *The Finite Element Method*, Prentice Hall, Englewood Cliffs, N.J., 1987.
- [15] W.F.Ames, *Numerical Methods for Partial Differential Equations*, Academic Press, New York, 1992.
- [16] W.H.Press, B.P.Flannery, S.A.Teukolsky, W.T.Vetterling, *Numerical Recipes*, Cambridge University Press, Cambridge, 1986.